Original Article

Computational Analysis of Selected Phytochemicals for their PARP Inhibitory Potential in Cancer

Mudassir Alam[1*], Kashif Abbas[1], Bharat Chaudhary[1], Sana Asif[1], Ali Asgar Balti[2]

[1] *Department of Zoology, Aligarh Muslim University, Aligarh, India. 202002*
[2] *Department of Biochemistry, Aligarh Muslim University, Aligarh, India. 202002*

Article info:
Received: 10 January 2024
Revised: 15 February 2024
Accepted: 25 February 2024

[*] **Corresponding Author:**

Mudassir Alam
Department of Zoology, Aligarh Muslim University, Aligarh, INDIA. 202002

Email: gh7949@myamu.ac.in

ABSTRACT

Poly (ADP-ribose) polymerase (PARP) inhibitors have emerged as promising agents in cancer prevention due to their ability to target the DNA repair machinery of cancerous cells. PARP enzymes repair single-strand DNA breaks through the base excision repair pathway. In cancer cells, particularly those with deficiencies in homologous recombination, PARP aids in DNA repair pathways and promotes cancer cell survival. PARP inhibitors suppress the enzyme function, thus inducing apoptosis in cancerous cells. Phytochemicals, bioactive compounds derived from plants, have gained increasing attention for their potential role in cancer prevention and treatment. We have investigated selected phytochemicals such as cinnamaldehyde, baicalein, curcumin, galangin, ellagic acid, resveratrol, pinocembrin, genistein, quercetin, and apigenin against PARP. The assessment of selected phytochemicals, including baicalein, galangin, ellagic acid, genistein, and apigenin, reveals promising attributes through various computational analyses. Specifically, these compounds exhibit favorable docking scores, indicating strong binding affinity to their target molecules. Molecular dynamic simulations for 10 nanoseconds were performed to validate the findings. Moreover, their potential as PARP inhibitors suggests a plausible role in inhibiting DNA repair mechanisms, an essential aspect of cancer therapy. These compounds were found to exert PARP inhibition through direct interference with enzymatic activity or modulation of PARP expression. This targeted investigation underscores the potential of these phytochemicals as PARP inhibitors, contributing to the advancement of precision cancer therapeutics.

Keywords: PARP, DNA repair, phytochemicals, cancer, molecular docking, MD simulation

Use your device to scan and read the article online

Citation: Alam M, Abbas K, Chaudhary B, Asif S, Balti AA. Computational Analysis of Selected Phytochemicals for their PARP Inhibitory Potential in Cancer. Acta Biochimica Iranica. 2024;2(1):11-21.

https://doi.org/***

Introduction

Cancer is a complex and often devastating group of diseases, characterized by the uncontrolled growth and spread of abnormal cells within the body. Around the world, approximately 17 million people are diagnosed with cancer every year (1). In recent years, there has been significant progress in the development of targeted cancer therapies, although conventional chemotherapy continues to be the primary approach for treating various types of cancer (2). Chemotherapeutic agents are designed to selectively target rapidly dividing cells. Nevertheless, a significant drawback of this treatment approach is its inability to differentiate between malignant and non-malignant cells (3). Patients undergoing chemotherapy frequently endure off-target toxicity and adverse side effects, as the chemotherapy drugs impact healthy tissues along with cancerous ones. The most common side effects are nausea and vomiting, with more than 90% of chemotherapy patients requiring anti-emetic drugs during cancer treatment (4). Patients also commonly report additional side effects such as fatigue, generalized pain, and various gastrointestinal disturbances. In contrast, targeted therapies aim at cancer-specific mutations and abnormalities to hinder tumor growth and progression while minimizing effects on surrounding non-malignant tissue. These therapies are frequently associated with more positive patient outcomes, as they are significantly less prone to causing off-target side effects (5). The Poly (ADP-ribose) polymerase (PARP) family consists of 17 members, alternatively referred to as the enzyme family ADP-ribosyl transferase diphtheria toxin-like (ARTD). These proteins are involved in several cellular processes like stress response, chromatin remodeling, DNA repair mechanism, and cell death, also known as apoptosis (6). The first member of the PARP protein family was identified in 1963 during research on an enzyme activated by nicotinamide mononucleotide (NMN) in a DNA-dependent manner. It was speculated to play a role in a reaction generating PolyA (7). The most widely acknowledged and extensively studied member of the PARP protein family is PARP1, initially recognized for its involvement in detecting and repairing single-strand DNA breaks (8). Recent findings indicate that PARP1 might also play a role in alternative DNA repair pathways, including nucleotide excision repair, classical and alternative non-homologous end joining, homologous recombination, and DNA mismatch repair (9). PARP inhibitors, often called PARPi, represent an innovative category of anti-cancer treatments. These inhibitors compete with NAD+ for the catalytically active site of PARP molecules and have demonstrated efficacy in treating various cancer types (10). PARP1 exhibits Poly (ADP-ribose) activity, and upon activation triggered by DNA damage, it synthesizes branched PAR chains. This process is crucial for recruiting additional repair proteins, facilitating the repair of DNA single-strand breaks (11). Significantly, PARPi marked a significant advancement as the first cancer drugs to specifically target the DNA damage response, particularly in breast and ovarian cancers with BRCA1/2 mutations (12). Over time, our comprehension of the mechanisms underlying tumor sensitization to PARP inhibitors has significantly advanced. Additionally, there has been an expansion in the application of PARPi to treat various other types of cancers, showcasing substantial progress in this field. Phytochemicals have garnered attention for their potential role in cancer (13), and various other ailments such as hypertension (14), diabetes (15), and several neurological disorders (16). The current study suggests virtually screening top phytochemicals with potential anticancer effects of phytoconstituents. The goal is to identify effective PARP-1 inhibitors using computational methods. The Naturally Occurring Plant-Based Anticancerous compound Activity Target (NPACT) database includes 1574 entries providing comprehensive information on the structure, physical attributes, elemental composition, topological properties, in vitro and in vivo biological activities, cancer types, cell lines, inhibitory values, molecular targets, commercial suppliers, and drug likeness of naturally occurring plant-based anticancer compounds (17). The study aims to evaluate phytochemicals for their potency as PARP inhibitors against 4RV6 protein (Human ARTD1 (PARP1) catalytic domain in complex with inhibitor Rucaparib). We employed various computational techniques to elucidate and evaluate the efficacy of these phytochemicals. Various computational approaches including molecular docking, molecular dynamic simulation, physicochemical properties, pharmacokinetics, absorption, distribution, metabolism, toxicological, and biological activity prediction were taken into consideration.

Material and Methods

Phytoconstituent data

Phytoconstituents, predominantly flavonoids and polyphenols, were compiled from the NPACT database (https://crdd.osdd.net/raghava/npact). All these drugs have been documented for their anticancer activities. The phytochemicals chosen for the study are given in Figure 1.

Protein preparation

The investigation utilized the Protein Database (https://www.rcsb.org/) to retrieve the PDB file corresponding to the Human ARTD1 (PARP1) catalytic domain in complex with the inhibitor Rucaparib, identifiable by its distinctive PDB ID: 4RV6. The Protein Data Bank

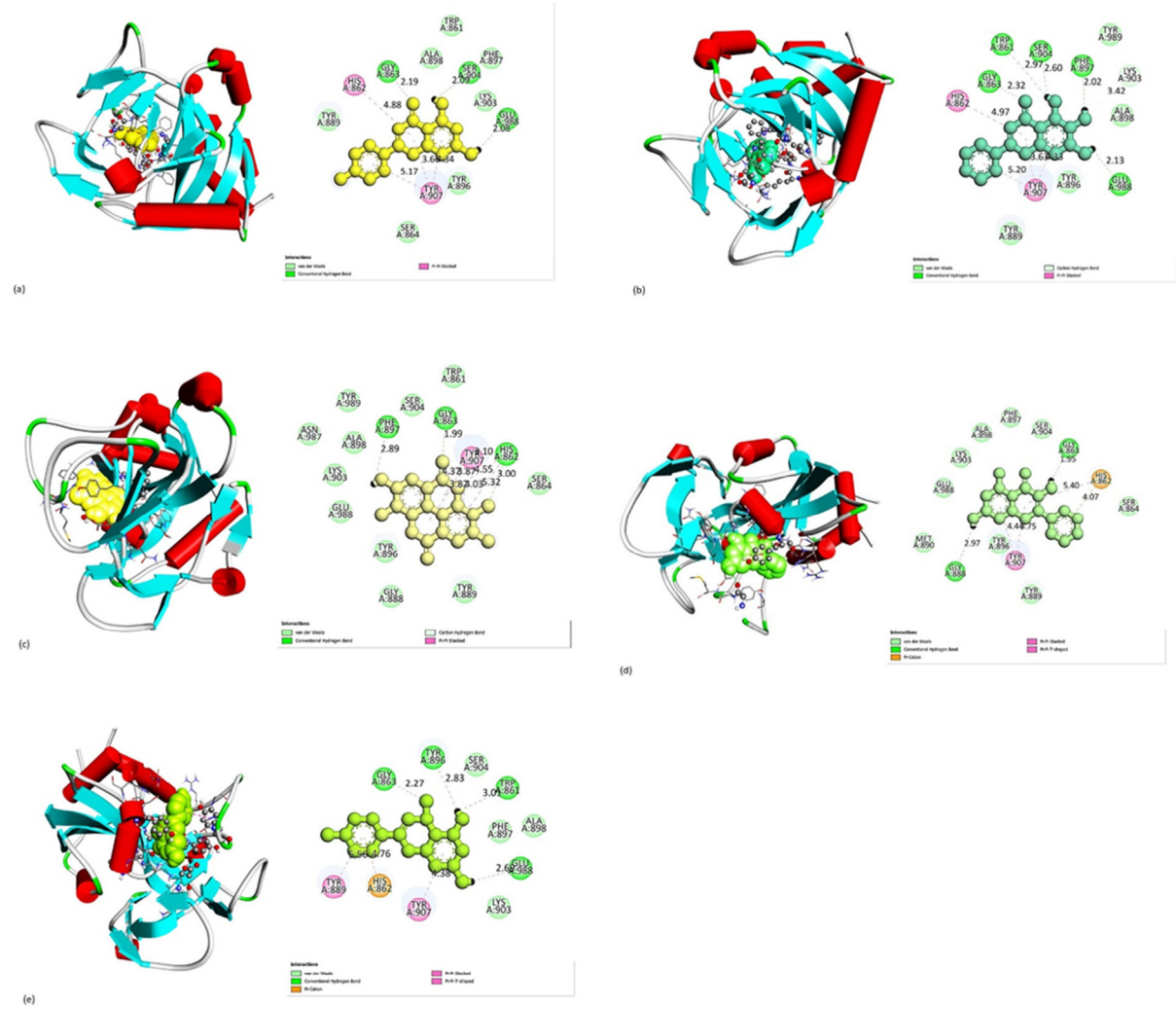

Figure 1: 2D representation of protein-ligand interaction of top five hit compounds: (a) Apigenin (b) Baicalein (c) Ellagic acid (d) Galangin (e) Genistein

(PDB) is an extensive repository containing information on experimentally determined structures of proteins and nucleic acids. In the subsequent stages of analysis, protein preparation procedures were executed, involving the elimination of water molecules and the bound ligand, Rucaparib. This task was efficiently executed using PyMOL (18), an open-source software tool renowned for its proficiency in generating molecular visualizations. The strategic use of PyMOL rendered it an optimal choice for facilitating the docking preparation process.

Ligand retrieval and preparation

The molecular structures of selected phytochemicals were acquired in sdf file format from the PubChem database, a valuable repository offering comprehensive information on chemical compounds, including structures, formulas, and molecular weights. In the ligand preparation phase for subsequent analysis, we employed the OpenBabel tool (19) within PyRx 0.8 (20). OpenBabel is a widely utilized software tool in molecular docking studies for ligand preparation. The ligand energy was minimized utilizing the mmff94 force field, a method chosen for its effectiveness in achieving stable and dependable ligand structures. Subsequently, the ligands' sdf file format was converted to pdbqt format, rendering the ligands executable and poised for docking. This conversion step was pivotal in ensuring compatibility and streamlining the subsequent molecular modeling and exploration of ligand-receptor interactions.

Molecular Docking

Molecular docking analysis investigated the interactions between chosen phytochemicals, serving as ligands, and the PARP-1 catalytic domain, the designated target macromolecule. In this study, we utilized the AutoDock Vina (21) tool, integrated into PyRx 0.8, to execute molecular docking. This facilitated a thorough

examination of conceivable binding interactions between the ligands and the macromolecule, providing valuable insights into their binding affinities and orientations.

Visualization of Docking Results

After conducting molecular docking, we identified the protein-ligand complex with the most favorable negative score, indicating a strong affinity. We selected this optimal binding pose for further analysis using Discovery Studio 4.5 (22). This software allowed us to visualize and explore the binding mode, enabling a detailed examination of ligand-receptor interactions. This in-depth analysis revealed critical molecular interactions that govern the ligand's high binding affinity to the PARP-1 catalytic domain.

Molecular dynamic simulation

Molecular dynamics (MD) simulations were conducted on the PARP-1 catalytic domain in the presence of selected phytochemicals, including apigenin, baicalein, ellagic acid, galangin, and genistein. The simulations were performed utilizing the WEBGRO Macromolecular Simulations server (https://simlab.uams.edu/ProteinWithLigand/protein_with_ligand.html), a public service provided by the University of Arkansas for Medical Sciences (UAMS) through the GRACE High-Performance Computing Facility. Before MD simulations, molecular topologies for the specified compounds were generated using the GlycoBioChemPRODRG2 server (http://davapc1.bioch.dundee.ac.uk/cgi-bin/prodrg). The GORMOS96 43A1 force field was employed for MD simulations of the PARP-1 catalytic domain with the identified compounds, employing the SPC water model within a triclinic system and sodium chloride. Subsequently, energy minimization of the formed complexes was carried out using a steepest descent integrator with steps performed at every 5000 intervals. Equilibration under NVT/NPT conditions at 300 K and 1 bar pressure followed this. The MD simulations were conducted with a Leap-frog integrator, spanning a simulation time of 10 ns, constrained by the available resources. A fixed frame count of 1000 frames was established. The trajectories obtained from MD simulations included root-mean-square deviation (RMSD), root-mean-square fluctuation (RMSF), radius of gyration (Rg), and solvent-accessible surface area (SASA). These parameters were analyzed at 300 K to gain insights into the complex formation dynamics (23, 24, 25). Utilizing these simulation techniques enhances our understanding of the interactions between the PARP-1 catalytic domain and the selected phytochemicals, contributing valuable information for further research in this domain.

Prediction of Physiochemical Properties

The physicochemical properties of the compounds were analyzed using the SWISS ADME webserver (26). This assessment involved the determination of various parameters crucial for characterizing the drug-likeness of a compound, including topological polar surface area (TPSA), xlogp3 (lipophilicity), logS (solubility), the number of hydrogen acceptors, the number of hydrogen donors, and molecular weight. Furthermore, instances where the compounds violated Lipinski's rule of five (27) were identified. Lipinski's rule of five delineates the essential criteria that orally active drugs must satisfy to demonstrate their pharmacological effectiveness.

Prediction of absorption, metabolism and distribution

The evaluation of predictions related to absorption, distribution, and metabolism for the selected compound was conducted using admetSAR (28). An online tool, accessible at http://lmmd.ecust.edu.cn/admetsar2/, was used to analyze various parameters. These parameters played a pivotal role in the prediction process, enhancing our comprehensive understanding of the compound's absorption, distribution, and metabolism attributes.

Prediction of toxicity

The chosen compound's toxicity was evaluated using ProTox-II (https://tox-new.charite.de/protox_II/index.php?site=compound_input) (29). This online platform functions as a virtual toxicity laboratory, facilitating the prediction of diverse toxicological outcomes linked to a chemical's structure. ProTox-II is accessible to both academic and non-commercial users. The system utilizes computer models trained on empirical data from in vitro or in vivo experiments to anticipate potential hazards associated with existing and hypothetical substances.

Prediction of biological activity of the compound

We employed the PASS web server to forecast the biological actions of the chosen molecules (http://www.pharmaexpert.ru/passonline) (30). Leveraging complex atom neighbor descriptors, the PASS analysis assists in elucidating a drug's effects solely based on its molecular formula, emphasizing that its biological function is intricately linked to its chemical arrangement..

Results and discussion

Docking score of the compounds

The docking study involved utilizing the 3D crystal structure of the PARP-1 catalytic domain, identified by PDB ID: 6NRF. Autodock Vina, accessed through PyRx

Table 1: Compounds with their molecular weight (MW), PUBCHEM ID and docking score

Name	MW (g/mol)	PUBCHEM ID	Docking Score (kcal/mol)
Cinnamaldehyde	132.16	637511	-6.0
Baicalein	270.24	5281605	-9.3
Curcumin	368.4	969516	-8.8
Galangin	270.24	5281616	-9.0
Ellagic Acid	302.19	5281855	-10
Resveratrol	228.24	445154	-8.0
Pinocembrin	256.25	68071	-8.9
Genistein	270.24	5280961	-10.5
Quercetin	302.23	5280343	-9
Apigenin	270.24	5280443	-9.2

Table 2: Interaction between phytochemicals present in berberis extract with amino acids of active site of PARP-1 catalytic domain

Ligand name	Interaction	Amino acids	Bond length (Å)
Baicalein	Van der Waals	Tyr889, Tyr896, Ala898, Tyr989	**----**
	Carbon-hydrogen bond	Lys903	**3.42**
	Pi-pi	His862, Tyr907	**4.97, 3.63**
	Hydrogen bond	Trp861, Gly863, Phe897, Ser904, Glu988	**2.97, 2.32, 2.02, 2.60, 2.13**
Galangin	Van der Waals	Ser864, Tyr889, Met890, Tyr896, Phe897, Ala898, Lys903, Ser904, Glu988	**----**
	Pi-pi	Tyr907	**4.44**
	Pi-cation	His862	**5.40**
	Hydrogen bonding	Gly863, Gly888	**1.95, 2.97**
Ellagic acid	Van der Waals	Trp861, Ser864, Gly888, Tyr889, Tyr896, Ala898, Lys903, Ser904, Asn987, Gly988, Tyr989,	**----**
	Pi-pi	Tyr907	**4.37**
	Hydrogen bond	His862, Glu863, Phe897	**3.00, 1.99, 2.89**
Genistein	Van der Waals	Phe897, Ala898, Lys903, Ser904	**----**
	Pi-pi	Tyr889, Tyr907	**5.50, 4.38**
	Hydrogen bond	Trp861, Gly863, Tyr896, Glu988	**3.01, 2.27, 2.83, 2.69**
	Pi-cation	His862	**4.76**
Apigenin	Van der Waals	Trp861, Ser864, Tyr896, Phe897, Tyr899, Lys903	**----**
	Pi-pi	His862, Tyr907	**4.88, 3.60**
	Hydrogen bond	Gly863, Ser904, Glu988	**2.19, 2.09, 2.08**

0.8, served as the tool for analysis. To prepare both the protein and the ligand for docking, UCSF Chimaera's Dockprep feature was employed. The protein was transformed into a macromolecule, and the chosen compounds underwent initial minimization using the mmff94 force field. Subsequently, the compounds were converted to pdbqt format using OpenBabel within PyRx. For the docking procedure, a grid box with dimensions of 59.95 Å × 42.18 Å × 41.10 Å was employed, centered at coordinates (25.40, -4.20, 18.63). The exhaustiveness level was set to the default value of 8. Specific details regarding the ligands or compounds and their respective docking scores are provided in Table 1. The most favorable docking poses of the top five phytochemicals and their interactions with the target protein are visually represented in Figure 1(a-e). Remarkably, each of the chosen compounds demonstrated promising docking scores, indicating their potential efficacy in binding to the PARP-1 catalytic domain.

Protein-ligand interaction

The top five distinct ligands—baicalein, galangin, ellagic acid, genistein, and apigenin—show various forms of interaction with the target protein. Baicalein is discerned to engage in Van der Waals interactions with the amino acids Tyr889, Tyr896, Ala898, and Tyr989. A Carbon-hydrogen bond manifests with Lys903, characterized by a bond length of 3.42 Å. Pi-pi interactions are evident with His862 and Tyr907, featuring bond lengths of 4.97 Å and 3.63 Å, respectively. Furthermore, Baicalein establishes Hydrogen bonds with Trp861, Gly863, Phe897, Ser904, and Glu988, each distinguished by discrete bond lengths—2.97 Å, 2.32 Å, 2.02 Å, 2.60 Å, and 2.13 Å respectively. The analogous patterns observed across the other ligands are noteworthy. For instance, Galangin participates in Van der Waals interactions with a spectrum of amino acids and conjoins Pi-pi interactions with Tyr907 (4.44

Å) and Pi-cation interactions with His862 (5.40 Å). Simultaneously, it engages in Hydrogen bonds with Gly863 (1.95 Å) and Gly888 (2.97 Å). Ellagic acid, on the other hand, interfaces through Van der Waals forces, Pi-pi interactions with Tyr907 (4.37 Å), and Hydrogen bonds with His862 (3.00 Å), Glu863 (1.99 Å), and Phe897 (2.89 Å). Genistein encompasses Van der Waals interactions, Pi-pi interactions with Tyr889 (5.50 Å) and Tyr907 (4.38 Å), Hydrogen bonds with Trp861 (3.01 Å), Gly863 (2.27 Å), Tyr896 (2.83 Å), and Glu988 (2.69 Å), alongside a Pi-cation interaction with His862 (4.76 Å). Similarly, Apigenin demonstrates Van der Waals interactions, Pi-pi interactions with His862 (4.88 Å) and Tyr907 (3.60 Å), and Hydrogen bonds with Gly863 (2.19 Å), Ser904 (2.09 Å), and Glu988 (2.08 Å). Table 2 summarizes the interaction between the binding site of the target protein and selected phytochemicals.

Molecular dynamic (MD) simulation

Molecular dynamics (MD) simulation is indeed a powerful methodology for modeling the entire protein-ligand system over a specific timeframe to examine conformational fluctuations (31). This technique employs Newton's law of motion in the macromolecular system, generating courses through the simulation span. Analysis of trajectory coordinates allows examination of constraints defining the stability of the protein-ligand complex (32, 33, 34). Trajectories such as Rg, RMSD, RMSF, and SASA for the PARP were graphed in the presence of apigenin, baicalein, ellagic acid, galangin, and genistein at 300 K. The investigation into overall changes in the structure of PARP primarily focused on the RMSD of primary chain atoms of PARP, depicting deviations from the initial positions or coordinates of the prepared protein molecule. Alternatively, structural modifications could be assessed by investigating the protein's Rg during small-angle X-ray scattering studies. The Rg serves as a constraint for assessing the stability of a molecular ensemble based on trajectory markers derived from MD simulations. It signifies the distance from the rotation axis to the center of mass. As indicated by Rg, structural constancy is characterized by reduced fluctuations in Rg values, signifying more excellent

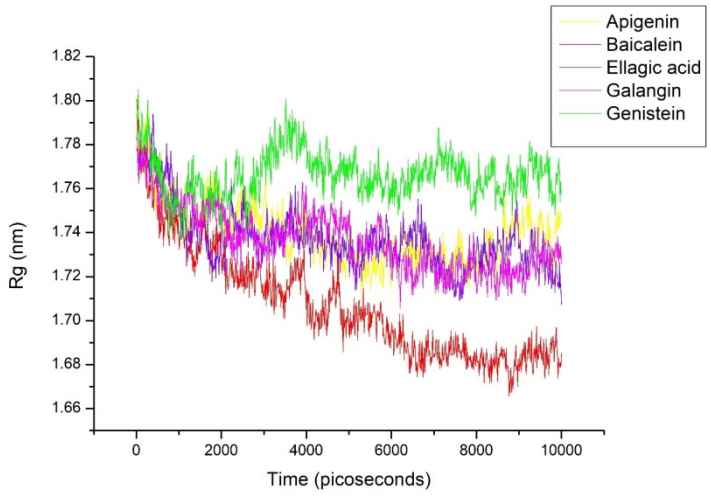

Figure 2: Radius of gyration study plot for 10 nanoseconds MD Simulation: apigenin (yellow), baicalein (red), ellagic acid (purple), galangin (magenta), and genistein (light green)

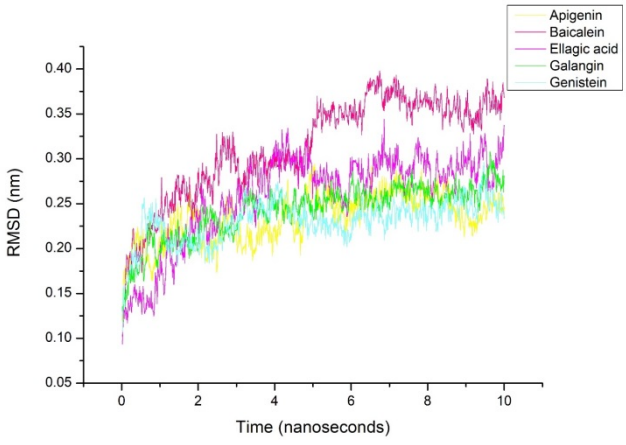

Figure 3: RMSD evaluation plot for 10ns: apigenin (yellow), baicalein (pink), ellagic acid (magenta), galangin (light green), genistein (light blue)

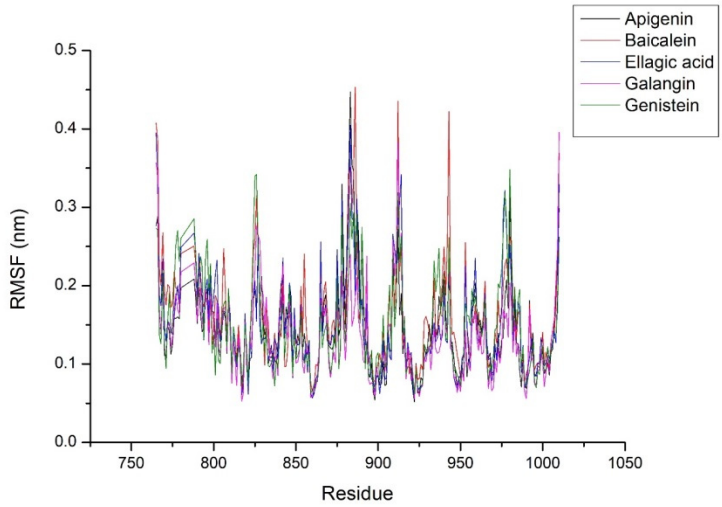

Figure 4: RMSF evaluation plot for 10ns: apigenin (black), baicalein (red), ellagic acid (blue), galangin (magenta), genistein (green)

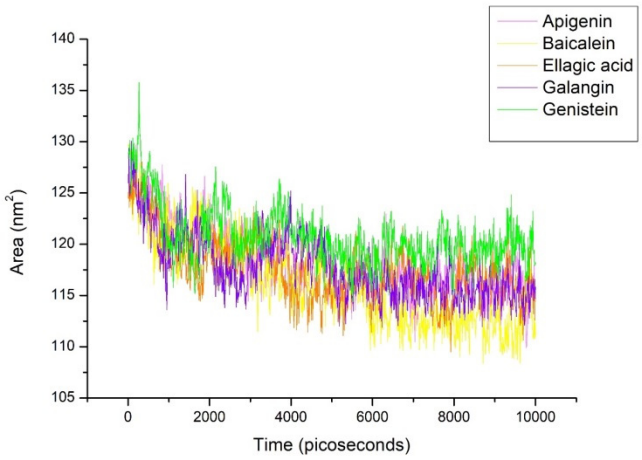

Figure 5: Solvent accessible surface area study plot for 10 ns MD Simulation: apigenin (purple), baicalein (yellow), ellagic acid (orange), galangin (blue), genistein (green)

stability in the protein-ligand complex. A smaller mean Rg value indicates the system is more tightly packed and exhibits a more compact overall structure. Figure 2 provides insights into the Rg of the ligand-protein complex at temperatures of 300 K. After simulating MD simulations for 10 ns, the least Rg values are found for apigenin, ellagic acid, and galangin, suggesting effective inhibition.

RMSD is indeed an alternative method for assessing a protein's stability following the conformational adaptation of the ligand. Using this methodology, the RMSD is derived by extracting atomic coordinates from the trajectories with a specific emphasis on backbone atoms. The calculation involves taking the square root of the mean value of the squares of these atomic positions. Decreased variability in the RMSD values for the complex signifies enhanced stability, and an RMSD value within the range of 3 angstroms indicates successful docking or fitting. It is essential to examine the RMSD of PARP with selected compounds (see Fig. 3). The plots reveal that the highest RMSD value was recorded for the baicalein-PARP complex, while the genistein-PARP showed the lowest RMSD value. The first stable conformation was attained at 7 ns with no considerable deviations in the values.

RMSF is a valuable metric for characterizing the conformational stability of a macromolecular system. Similar to RMSD, it is determined by measuring the mean square root of the atomic positions, but in this case, it focuses on individual residue flexibility. Reduced coordinate fluctuation signifies more excellent stability, and symmetrical fluctuation indicates more constancy than asymmetrical variation. When plotting RMSF values for the protein-ligand complex, mainly focusing on fluctuations in specific regions, it provides insights into the induced fitting of the ligand. As depicted in Figure 4, it is evident that there is symmetrical fluctuation when MD simulations are conducted. Consequently, the complex exhibits stability, suggesting inhibition of PARP.

Table 3: Physiochemical properties of chosen phytochemicals

Ligand Name	MW	PUBCHEM ID	LogS	Logo /w	Accept H	Donor H	TPSA (Å)	GI absorption	Drug-likeness
Baicalein	270.24	5281605	-4.03	3.16	5	3	90.90	High	**YES**
Galangin	270.24	5281616	-3.41	2.25	5	3	90.90	High	**YES**
Ellagic Acid	302.19	5281855	-2.94	1.10	8	4	141.34	High	**YES**
Genistein	270.24	5280961	-3.72	2.67	5	3	90.90	High	**YES**
Apigenin	270.24	5280443	-3.94	3.02	5	3	90.90	High	**YES**

Table 4: Absorption, distribution, and metabolism of the selected compound out of all docked compound as per admetSAR online toolkit

Parameters	Baicalein (1)	Galangin (2)	Ellagic acid (3)	Genistein (4)	Apigenin (5)
ABSORPTION					
Human oral bioavailability	Positive	Negative	Positive	Negative	Negative
Human intestinal absorption	Positive	Positive	Positive	Positive	Positive
P-glycoprotein substrate	Negative	Negative	Negative	Negative	Negative
P-glycoprotein inhibitior	Negative	Negative	Negative	Negative	Negative
DISTRIBUTION					
Subcellular localization	Mitochondria	Mitochondria	Mitochondria	Mitochondria	Mitochondria
METABOLISM					
CYP2C9 substrate	Non-substrate	Non-substrate	Non-substrate	Non-substrate	Non-substrate
CYP2D6 substrate	Non-substrate	Non-substrate	Non-substrate	Non-substrate	Non-substrate
CYP3A4 substrate	Non-substrate	Non-substrate	Non-substrate	Non-substrate	Non-substrate
CYP1A2 inhibition	Inhibitor	Inhibitor	Non-inhibitor	Inhibitor	Inhibitor
CYP2C9 inhibition	Non-inhibitor	Inhibitor	Non-inhibitor	Inhibitor	Inhibitor
CYP2D6 inhibition	Non-inhibitor	Non-inhibitor	Non-inhibitor	Non-inhibitor	Non-inhibitor
CYP2C19 inhibition	Non-inhibitor	Inhibitor	Non-inhibitor	Inhibitor	Inhibitor

The average SASA value was determined to be approximately 138 nm², falling within the range of 150–130 nm². In the case of the NAR complex, a similar trend was observed; with a trajectory showing a decrease in values up to 10 ns, followed by minor fluctuations during the simulation period (Fig. 5). The average SASA value for the NAR complex was approximately 118 nm², ranging between 108–135 nm². Notably, the baicalein-PARP complex displayed the lowest average SASA, while the genistein-PARP complex exhibited the highest SASA average.

Evaluation of pharmacological and toxicological properties

The assessment of drug-likeness in the top five phytochemicals through an analysis of ADME/T properties was done using the SWISSADME webserver. This encompassed applying drug similarity rules, including Lipinski's rule, to discern suitable compounds. The summarized outcomes are presented in Tables 3 and 4, with the latter offering insights into the anticipated absorption, distribution, and metabolism via the admetSAR server. The pivotal criteria influencing a compound's potential as a drug candidate, encompassing topological polar surface area (TPSA), molecular weight (MW), logS (solubility), and xlog3 value, were considered.

Baicalein, with a molecular weight of 270.24, demonstrates notable properties in the molecular profile. Its LogS of -4.03 suggests high solubility and a LogP of 3.16 indicates a tendency for lipophilic interactions. The molecule has five hydrogen bond acceptors and three donors, contributing to its moderate hydrogen bonding capacity. Baicalein exhibits high gastrointestinal absorption potential, and its drug-likeness is affirmed.

Galangin, sharing the same molecular weight of 270.24, exhibits distinct characteristics. A LogS of -3.41 maintains good solubility, and a LogP of 2.25 signifies moderate lipophilicity. Similar to Baicalein, Galangin has five hydrogen bond acceptors and three donors. It is classified as having high gastrointestinal absorption

Table 5: Toxicological prediction of the compounds using PROTOX- II server

Parameters	Baicalein	Galangin	Ellagic acid	Genistein	Apigenin
Carcinogenicity	Weak/low	Inactive	Weak/low	Inactive	Inactive
Mutagenicity	Weak/low	Inactive	Inactive	Inactive	Inactive
Cytotoxicity	Inactive	Inactive	Inactive	Inactive	Inactive
Immunotoxicity	Inactive	Inactive	Inactive	Inactive	Inactive
Androgen receptor	Inactive	Inactive	Inactive	Inactive	Inactive

Table 6: Biological activity prediction of compounds (Pa = probability to be active; Pi = probability to be inactive)

Compound name	Biological activity	Pa	Pi
Baicalein		0.230	0.017
Galangin		0.134	0.055
Ellagic acid		0.194	0.027
Genistein	**PARP inhibitor**	0.164	0.038
Apigenin		0.149	0.045

potential, and its drug-likeness is also affirmed.

Ellagic Acid, with a slightly larger molecular weight of 302.19, presents unique features. Its LogS of -2.94 indicates comparatively lower solubility and a LogP of 1.10 suggests a more hydrophilic nature. Ellagic Acid has eight hydrogen bond acceptors and four donors, indicating a higher potential for hydrogen bonding interactions. With a TPSA of 141.34 Å, it possesses a larger polar surface area. Despite lower solubility, ellagic acid is classified as having high gastrointestinal absorption potential and is drug-like.

Genistein, like Baicalein and Galangin, has a molecular weight of 270.24. Its LogS of -3.72 indicates moderate solubility and a LogP of 2.67 suggests moderate lipophilicity. With five hydrogen bond acceptors and three donors, Genistein shares a hydrogen bonding profile similar to that of Baicalein and Galangin. It is categorized as having high gastrointestinal absorption potential and showed drug-likeness.

With a molecular weight of 270.24, Apigenin aligns with its counterparts in certain aspects. It has a LogS of -3.94, indicating moderate solubility and a LogP of 3.02, suggesting a preference for lipophilic environments. With five hydrogen bond acceptors and three donors, Apigenin shares a hydrogen bonding profile similar to Baicalein, Galangin, and Genistein. Apigenin is classified as having high gastrointestinal absorption potential and exhibits drug-likeness.All the chosen phytochemicals have shown drug-likeness properties.

The toxicity prediction of compounds was indeed conducted using the Protox II server, and the findings are outlined in Table 5. The toxicity prediction results for five compounds—Baicalein, Galangin, Ellagic acid, Genistein, and Apigenin—were assessed using the Protox II server.

Regarding carcinogenicity, baicalein exhibited a weak/low level, and ellagic acid showed weak/low activity, while galangin, Genistein, and apigenin were classified as inactive. Similarly, mutagenicity assessments revealed Baicalein to be weak/low, while Galangin, Ellagic acid, Genistein, and Apigenin were all inactive.

Across the board, the compounds demonstrated inactivity in cytotoxicity, immunotoxicity, and androgen receptor activity. Specifically, Baicalein, Galangin, Ellagic acid, Genistein, and Apigenin were inactive in these categories, indicating a lack of toxicity concerning these parameters.

This comprehensive analysis provides valuable insights into the toxicity profiles of the compounds, aiding in a better understanding of their safety considerations in various contexts.

Predictions of Biological Activity of Compounds

The PASS webserver was indeed utilized to validate the anticipated biological effects. All five chosen compounds—Baicalein, Galangin, Ellagic acid, Genistein, and Apigenin—possess the ability to inhibit PARP. The Pa values for PARP inhibitor range between 0.134 to 0.230, while for Pi, the value ranged between 0.017 and 0.055. When the Pa value surpasses the Pi value, it indicates a probable presence of the specified biological activity. The summarized outcomes are presented in Table 6.

Conclusion

Your investigation indeed highlights the considerable promise of baicalein, galangin, ellagic acid, genistein, and apigenin as PARP inhibitors through various computational investigations, including molecular docking and MD simulation for 10 ns. The systematic use of computational tools has identified these phytochemicals as viable candidates and elucidated their molecular interactions with the target protein, thereby confirming their robust binding affinity. The favorable drug-likeness characteristics and reassuring safety profiles further underscore their suitability for therapeutic development. While your computational findings establish a solid foundation, it is indeed crucial

to emphasize the imperative of empirical validation through wet lab trials. The transition from virtual predictions to experimental verification is pivotal in affirming the efficacy of these phytochemicals and establishing their potential as PARP inhibitors in practical applications

Acknowledgement

The authors would like to acknowledge Prof. Nazura Usmani's laboratory, Department of Zoology, Aligarh Muslim University, for providing the facilities required for the work.

Competing interest

Authors declares no conflict of interest.

Funding disclosure

Authors declare that they have not received any funding for this work.

References

1. Mustafa M, Abbas K, Alam M, Ahmad W, Moinuddin, Usmani N, et al. Molecular pathways and therapeutic targets linked to triple-negative breast cancer (TNBC). Mol Cell Biochem. 2023:1-19. https://doi.org/10.1007/s11010-023-04772-6
2. Pérez-Herrero E, Fernández-Medarde A. Advanced targeted therapies in cancer: Drug nanocarriers, the future of chemotherapy. Eur J Pharm Biopharm. 2015;93:52-79. https://doi.org/10.1016/j.ejpb.2015.03.018
3. Joo WD, Visintin I, Mor G. Targeted cancer therapy-are the days of systemic chemotherapy numbered? Maturitas. 2013;76(4):308-314. https://doi.org/10.1016/j.maturitas.2013.09.008
4. Herrstedt J, Dombernowsky P. Anti-emetic therapy in cancer chemotherapy: current status. Basic Clin Pharmacol Toxicol. 2007;101(3):143-150. https://doi.org/10.1111/j.1742-7843.2007.00122.x
5. Schmitt CA, Wang B, Demaria M. Senescence and cancer-role and therapeutic opportunities. Nat Rev Clin Oncol. 2022;19(10):619-636. https://doi.org/10.1038/s41571-022-00668-4
6. Jubin T, Kadam A, Jariwala M, Bhatt S, Sutariya S, Gani AR, et al. The PARP family: insights into functional aspects of poly (ADP-ribose) polymerase-1 in cell growth and survival. Cell Prolif. 2016;49(4):421-437. https://doi.org/10.1111/cpr.12268
7. Hassa PO, Haenni SS, Elser M, Hottiger MO. Nuclear ADP-ribosylation reactions in mammalian cells: where are we today and where are we going? Microbiol Mol Biol Rev. 2006;70(3):789-829. https://doi.org/10.1128/MMBR.00040-05
8. Thomas C, Tulin AV. Poly-ADP-ribose polymerase: machinery for nuclear processes. Mol Aspects Med. 2013;34(6):1124-1137. https://doi.org/10.1016/j.mam.2013.04.001
9. De Vos M, Schreiber V, Dantzer F. The diverse roles and clinical relevance of PARPs in DNA damage repair: current state of the art. Biochem Pharmacol. 2012;84(2):137-146. https://doi.org/10.1016/j.bcp.2012.03.018
10. Javle M, Curtin NJ. The potential for poly (ADP-ribose) polymerase inhibitors in cancer therapy. Ther Adv Med Oncol. 2011;3(6):257-267. https://doi.org/10.1177/1758834011417039
11. Aberle L, Krüger A, Reber JM, Lippmann M, Hufnagel M, Schmalz M, et al. PARP1 catalytic variants reveal branching and chain length-specific functions of poly (ADP-ribose) in cellular physiology and stress response. Nucleic Acids Res. 2020;48(18):10015-10033. https://doi.org/10.1093/nar/gkaa590
12. Yi M, Dong B, Qin S, Chu Q, Wu K, Luo S. Advances and perspectives of PARP inhibitors. Exp Hematol Oncol. 2019;8:1-12. https://doi.org/10.1186/s40164-019-0154-9
13. Ranjan A, Ramachandran S, Gupta N, Kaushik I, Wright S, Srivastava S, Das H, Srivastava S, Prasad S, Srivastava SK. Role of Phytochemicals in Cancer Prevention. Int J Mol Sci. 2019;20(20):4981. https://doi.org/10.3390/ijms20204981
14. Pagliaro B, Santolamazza C, Simonelli F, Rubattu S. Phytochemical Compounds and Protection from Cardiovascular Diseases: A State of the Art. Biomed Res Int. 2015;2015:918069. https://doi.org/10.1155/2015/918069
15. Ajiboye BO, Iwaloye O, Owolabi OV, Ejeje JN, Okerewa A, Johnson OO, et al. Screening of potential antidiabetic phytochemicals from Gongronema latifolium leaf against therapeutic targets of type 2 diabetes mellitus: multi-targets drug design. SN Appl Sci. 2021;4(1):14. https://doi.org/10.1007/s42452-021-04880-2
16. Abbas K, Alam M, Ali V, Ajaz M. Virtual screening, molecular docking and ADME/T properties analysis of neuroprotective property present in root extract of chinese skullcap against β-site amyloid precursor protein cleaving enzyme 1 (BACE1) in case of alzheimer's disease. J Pharmacogn Phytochem. 2023;12(1):146-53.
17. Mangal M, Sagar P, Singh H, Raghava GP, Agarwal SM. NPACT: Naturally Occurring Plant-based Anti-cancer Compound-Activity-Target database. Nucleic Acids Res. 2013 J(Database issue):D1124-9. https://doi.org/10.1093/nar/gks1047
18. Schrödinger L, DeLano W. PyMOL. 2020. Available from: http://www.pymol.org/pymol
19. O'Boyle NM, Banck M, James CA, Morley C, Vandermeersch T, Hutchison GR. Open Babel: An open chemical toolbox. J Cheminform. 2011;3(1):1-4. https://doi.org/10.1186/1758-2946-3-33
20. Dallakyan S, Olson AJ. Small-molecule library screening by docking with PyRx. Chem Biol Methods Protoc. 2015:243-50. https://doi.org/10.1007/978-1-4939-2269-7_19
21. Trott O, Olson AJ. AutoDock Vina: improving the speed and accuracy of docking with a new scoring function, efficient optimization, and multithreading. J Comput Chem. 2010;31(2):455-61. https://doi.org/10.1002/jcc.21334
22. Discovery Studio Modeling Environment, Release 4.5. 2021. BIOVIA, Dassault Systèmes, San Diego.
23. Oostenbrink C, Villa A, Mark AE, van Gunsteren WF. A biomolecular force field based on the free enthalpy of hydration and solvation: the GROMOS force-field parameter sets 53A5 and 53A6. J Comput Chem. 2004(13):1656-76. https://doi.org/10.1002/jcc.20090
24. Abraham MJ, Murtola T, Schulz R, Páll S, Smith JC, Hess B, et al. GROMACS: High performance molecular simulations through multi-level parallelism from laptops to supercomputers. SoftwareX. 2015;1-2:19-25. https://doi.org/10.1016/j.softx.2015.06.001
25. Bjelkmar P, Larsson P, Cuendet MA, Hess B, Lindahl E. Implementation of the CHARMM Force Field in GROMACS: Analysis of Protein Stability Effects from Correction Maps, Virtual Interaction Sites, and Water Models. J Chem Theory Comput. 2010;6(2):459-66. https://doi.org/10.1021/ct900549r

26. Daina A, Michielin O, Zoete V. SwissADME: a free web tool to evaluate pharmacokinetics, drug-likeness and medicinal chemistry friendliness of small molecules. Sci Rep. 2017;7:42717. https://doi.org/10.1038/srep42717
27. Lipinski CA, Lombardo F, Dominy BW, Feeney PJ. Experimental and computational approaches to estimate solubility and permeability in drug discovery and development settings 1PII of original particle: S0169-409X(96)00423-1. Adv Drug Deliv Rev. 2001;46(1-3):3-26. https://doi.org/10.1016/S0169-409X(00)00129-0
28. Cheng F, Li W, Zhou Y, et al. AdMetSAR: a comprehensive source and free tool for assessment of chemical ADMET properties. J Chem Inf Model. 2012;52(11):3099-3105. https://doi.org/10.1021/ci300367a
29. Banerjee P, Eckert A, Schrey AK, Preißner R. ProTox-II: a webserver for the prediction of toxicity of chemicals. Nucleic Acids Res. 2018;46(W1):W257-W263. https://doi.org/10.1093/nar/gky318
30. Filimonov DA, Lagunin AA, Gloriozova TA, Rudik AV, Druzhilovskii DS, Pogodin PV, Poroikov VV. Prediction of the biological activity spectra of organic compounds using the PASS online web resource. Chem Heterocycl Compd. 2014;50:444-57. https://doi.org/10.1007/s10593-014-1496-1
31. Lindorff-Larsen K, Piana S, Palmo K, Maragakis P, Klepeis JL, Dror RO, Shaw DE. Improved side-chain torsion potentials for the Amber ff99SB protein force field. Proteins. 2010;78(8):1950-8. https://doi.org/10.1002/prot.22711
32. Meena P, Manral A, Nemaysh V, Saini V, Siraj F, Luthra P, et al. Novel Insights into Multitargeted Potential of N'-(4-benzylpiperidin-1-yl)alkylamine derivatives in the Management of Alzheimer's Disease Associated Pathogenesis. RSC Adv. 2016;6. https://doi.org/10.1039/C6RA24017H
33. Balasundaram A, Doss GPC. A computational examination of the therapeutic advantages of fourth-generation ALK inhibitors TPX-0131 and repotrectinib over third-generation lorlatinib for NSCLC with ALK F1174C/L/V mutations. Frontiers in Molecular Biosciences. 2024;10. https://doi.org/10.3389/fmolb.2023.1306046
34. Saah SA, Sakyi PO, Adu-Poku D, Boadi NO, Djan G, Amponsah D, et al. Docking and Molecular Dynamics Identify Leads against 5 Alpha Reductase 2 for Benign Prostate Hyperplasia Treatment. Journal of Chemistry. 2023;2023:8880213. https://doi.org/10.1155/2023/8880213